Determination of presence of undesirable carbides at surface of cast iron parts using differential eddy current technique

M. Kashefi[1] and S. Kahrobaee*[2]

Machinability of grey cast iron parts can greatly suffer from the formation of carbide at the surface, resulting in a decrease in cutting tool life and higher production costs. Therefore, detection of the hardened layer and its hardness are the key factors in quality control and inspection processes. In the present paper, a number of metallurgical parameters (surface carbide, surface hardness and hardened depth) have been investigated using the non-destructive differential eddy current technique. The results show the high potential of the proposed method as a fast and accurate technique in inspecting and in consequent separation of undesirable parts.

Keywords: Grey cast iron, Surface carbide, Hardened layer, Differential eddy current

Introduction

Considering the importance of dimensional precision, machinability is a main factor in mass production of cast iron parts. Machinability is broadly defined as the ability of the workpiece material to be machined.[1] Investigations conducted on cast iron have shown that machinability is directly related to the microstructure of the matrix surrounding the graphite nodules.[2–4] Generally, a ferritic matrix has the highest machinability, and a mixture of pearlite and free carbides shows the lowest one. Therefore, as the microstructure changes from ferrite to pearlite, the machinability and the cutting tool's life decrease. Formation of a thin surface layer consisting of hard carbides is a common difficulty in the machining of grey cast iron parts. This problem, particularly in the parts containing thin sections, is due to the improper design of the gating system and/or wrong choice of casting parameters such as pouring speed and temperature.[2,3] Formation of the mentioned layer reduces the cutting tool's life and restricts the machinability of the parts. As a result, detection of the occurrence and determination of the depth of this layer could be considered as a useful tool in the quality control of cast iron parts.

Traditional techniques used for detecting the carbide layer are metallographic examination and hardness testing, which are usually conducted after an appreciative decrease in the cutting tool's lifetime. These methods are costly and time consuming and could not be considered as preventive methods to prevent damage to the tools. Non-destructive evaluation techniques are proven to be fast, cost effective and in particular have the ability to be employed on each part separately.[5] Emerging techniques indicate the potential of the methods in various industrial fields' applications.[6] Eddy current (EC) testing is considered as an efficient and reliable method in microstructural evaluations such as determination of pearlite percentage,[7–9] austenitic phase variation induced by aging and cold working,[10,11] martensite content[12] and secondary phase precipitation,[13,14] as well as mechanical properties[15,16] in steel and cast iron parts. In addition to the tests conducted for bulk evaluation, surface characterisation such as determination of the decarburised layer thickness,[17–19] depth of the hardened layer in induction hardening[20,21] and surface carbon content of the carburised parts[22] has also been investigated. This indicates the great potential of this method in the detection of microstructural changes occurring at the surface of ferromagnetic parts.

In the present study, application of differential EC technique in determining the occurrence and the depth of the hardened layer due to the presence of the carbides in the surface of grey cast irons has been investigated.

Experimental

Six grey cast iron blocks with dimension of $40 \times 40 \times 30$ mm and composition of 3·47%C–1·96%Si–0·45%Mn–0·0026%P–0·014%S–0·016%Cr were used for the present study. Casting of all the samples was conducted in one step. In order to provide various cooling rates (layers with various surface carbide contents on the surface of the samples), cast iron chills with different thicknesses ranging from 4 to 20 mm were used as indicated in Fig. 1. Longitudinal sectioning of the samples was used for metallographic and hardness tests. Measurement of % surface carbide (using microscopic observation and Microstructure Image Processing software) and surface hardness values (as mean hardness up to depth of 500 μm) as well as hardness profiling were carried out for all samples.

[1]Department of Materials Science and Metallurgical Engineering, Engineering Faculty, Ferdowsi University of Mashhad, Mashhad, Iran
[2]Department of Materials Science and Metallurgical Engineering, Sadjad Institute of Higher Education, Mashhad, Iran

*Corresponding author, email kahrobaee@sadjad.ac.ir

Published by Maney on behalf of the Institute
Received 9 July 2012; accepted 6 March 2013
DOI 10.1179/1743284713Y.0000000243

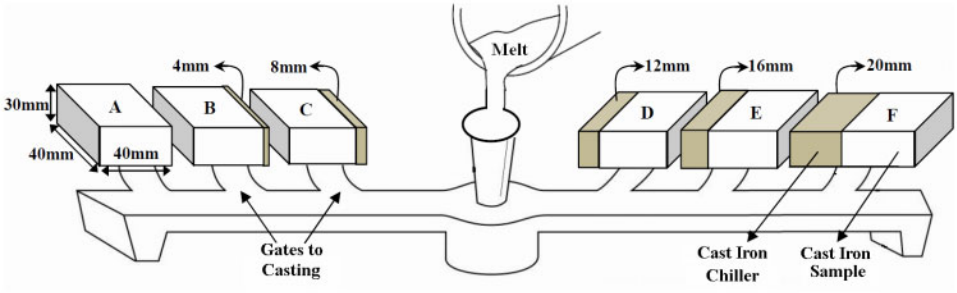

1 Schematic diagram of applied casting procedure

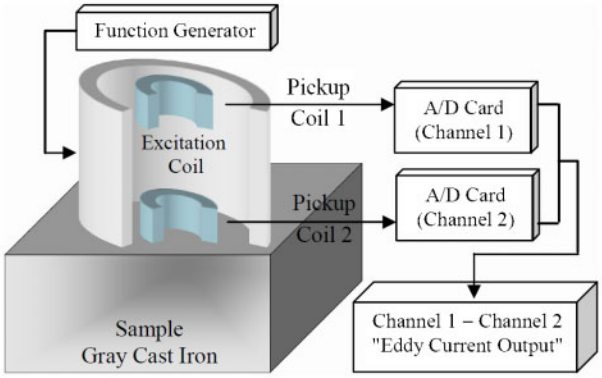

2 General synopsis of designed differential eddy current apparatus

Eddy current testing was applied to all the samples. The schematic diagram of the EC system used is shown in Fig. 2. The applied EC system consists of a function generator, a sinusoidal wave generator with varying duty cycle and frequency, a differential probe having excitation coil and two pick up coils, a sensitive difference amplifier that subtracts the outputs of the two pick up coils, an A/D converter and a computer with data acquisition. The differential probe consists of an excitation copper coil of 120 turns wound on a cylindrical ferrite core with dimensions of 22 mm inner and 26 mm outer diameter. To detect the EC response, two pick up coils were placed at the top and bottom axial centre of the excitation probe as shown in Fig. 2. The magnetic field detected by the two sensors was subtracted by a difference amplifier, and the resultant signal was used as the EC output. In order to determine an optimum frequency, EC tests were performed in the range of 100–1000 Hz. Finally, correlations between the destructive technique results and output data from non-destructive EC testing were established.

Results and discussion

Metallographic and hardness evaluations

Metallography and microstructural observations are traditional methods in detecting the surface microstructural changes of cast iron parts. Figure 3 shows the microscopic image of the hardened layer formed at the surface of sample 'B' in Fig. 1. As can be seen, graphite with D type (undercooled flake graphite) morphology at the core has changed to cluster form at the surface of the cast sample. Increasing the cooling rate at the surface can produce a mottled iron, in which carbon is present in the form of both primary cementite (iron carbide) and graphite. As a result, the microstructure at the surface consists of graphite (cluster black zones) and free cementite (white zones) in a pearlitic matrix.

Macro- and microetched images of the longitudinal sections for all samples have been depicted in Fig. 4. The hardened layers show different percentages of graphite, free cementite and pearlite as a result of different cooling (solidification) rates at the surface of the samples. The percentages of carbide, graphite and pearlite in the samples were measured using Microstructure Image Processing software and have been presented in Table 1.

Longitudinal hardness profile of the samples was also plotted using microhardness measurement (Fig. 5). As can be seen, there is a good agreement between the hardness profiles and microstructure at the surface of the samples. Furthermore, the hardness profiles show that in addition to the increase in the depth of the hardened layer obtained under more intense cooling conditions, the hardness in the surface layers has also been increased. This is due to an increase in the amount

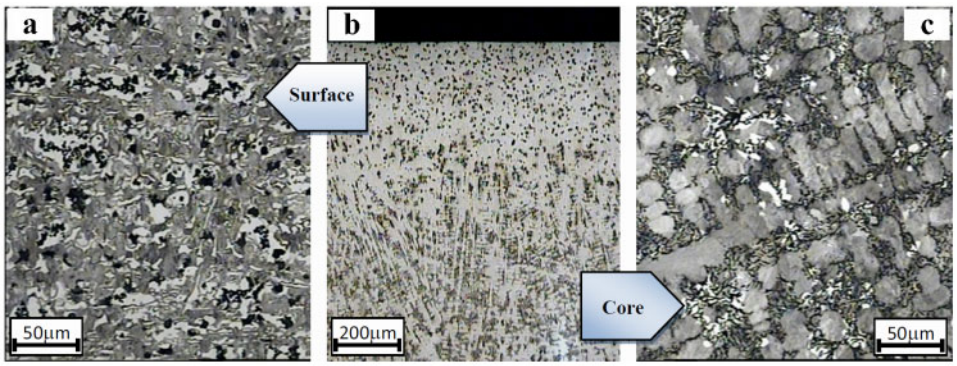

3 *a* microstructure of grey cast iron surface (free carbide, clustered graphite and pearlite), *b* macroetched image of surface (as polished) and *c* core (D type graphite and pearlite)

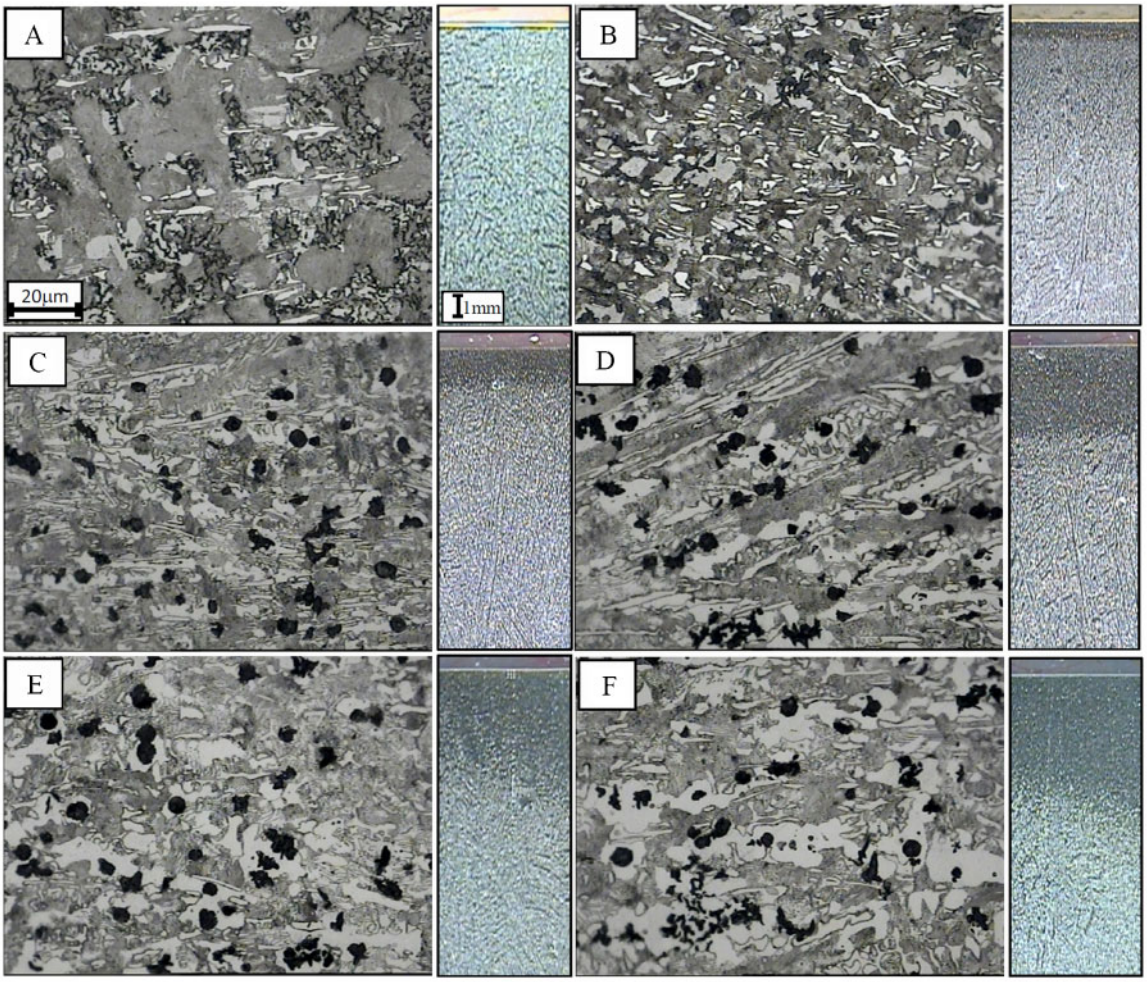

4 Microscopic and macroscopic images of samples A to F

of carbide at the surface layers resulting from a higher solidification rate. The results of hardness evaluations are also displayed in Table 1.

Non-destructive evaluation by EC method

In EC testing, an alternating current is applied to the excitation coil using a function generator. As a result, a primary alternating magnetic field, which is detectable by pick up coils, induces ECs in the test specimen. Thus, there are two parameters that affect the lower pick up coil. The first factor is the formation of a secondary magnetic field opposing the primary one. The second one is the magnetic flux density related to the amplification of the primary field, which is caused by placing a ferromagnetic material in the vicinity of the coil. Since the samples are ferromagnetic, they increase the magnetic flux density B in direct proportion to the magnetic permeability of the material $B \alpha \mu$. Therefore, amplification of the field has a dominant effect on the lower pick up coil in comparison with the opposing field. On the other hand, the upper pick up coil would only detect the magnetic field produced by the excitation coil. As a result, by subtraction the induced voltage of the upper and lower coils (net induced voltage), we could claim that the mentioned output is particularly affected by the magnetic properties of the samples. As a result, the effect of the field resulting from the excitation coil would be eliminated.[23,24]

Relations between EC output (net induced voltage) and metallurgical parameters

First, regression analysis was used to determine the optimum frequency. Considering a frequency ranging from 100 to 1000 Hz, the highest regression coefficient between EC outputs and surface carbide percentage was obtained at the frequency of 350 Hz. As a result, 350 Hz was considered as the optimum frequency, and all EC tests were conducted at this frequency.

Table 1 Measured phase percentage, surface hardness and hardened depth

Sample	A	B	C	D	E	F
Chill thickness/mm	0	4	8	12	16	20
Surface carbide percentage	5·89	7·10	18·46	24·25	28·82	31·27
Graphite percentage	13·39	15·91	7·08	9·34	8·78	7·10
Pearlite percentage	80·73	76·98	74·47	66·44	62·40	61·63
Surface hardness/HV	266	306	314	354	413	488
Hardened depth/μm	0	670	1300	3200	5050	5300

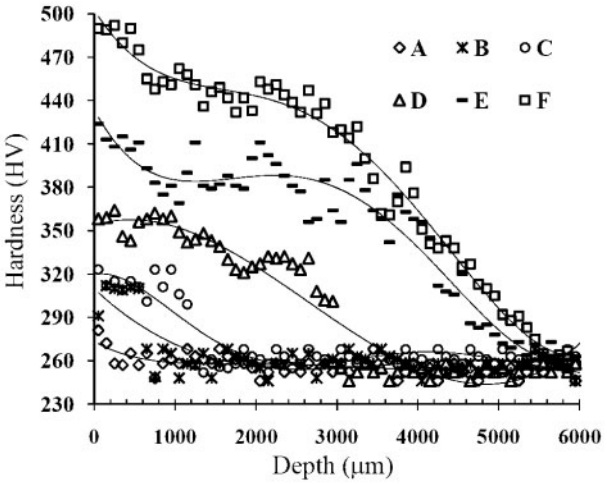

5 Measured hardness profiles of samples with different surface carbide contents

Figure 6 shows the relation between the EC outputs and the surface carbide percentage of the cast iron samples. The high regression coefficient (R^2=0·86) indicates the capability of the EC method to detect surface carbide percentage in the cast iron samples studied, and it is concluded that a higher surface carbide percentage causes a decrease in EC output (net induced voltage).

According to Table 1, it is clear that by increasing the thickness of the chill and, therefore, the cooling rate at the surface, the carbide percentage increases and pearlite (which contains the magnetically soft ferrite) fraction decreases with no significant change in graphite content. Thus, for sample A, with the highest fraction of pearlite, the highest magnetic flux density and coil reactance X_L can be obtained. On the other hand, carbide phase restricts electron flow and thus increases the electrical resistance R. Changes in X_L and R result in coil impedance and, therefore, induce voltage changes according to equation (1)

$$Z=\left(X_L^2+R^2\right)^{1/2}=V/I \tag{1}$$

Since in ferromagnetic materials the effect of permeability or reactance is stronger than the effect of resistance,[25,26] by increasing the carbide content in the

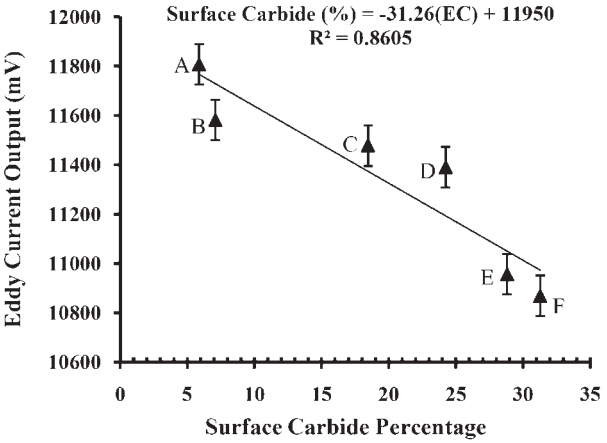

6 Relationship between EC output and surface carbide content

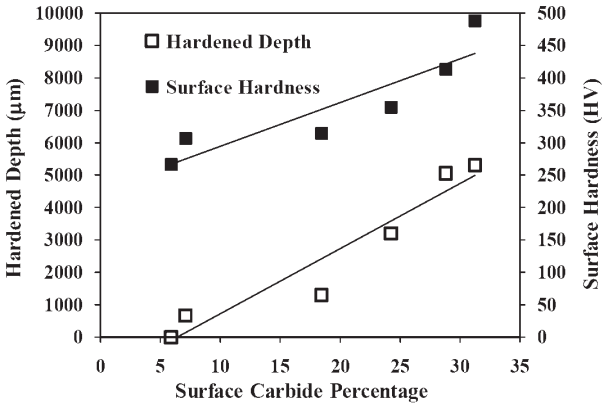

7 Linear relations between carbide content, surface hardness and hardened depth

samples, coil impedance and induced voltage decrease, as seen in Fig. 6. Thus, a direct relation can be established between microstructural and electromagnetic properties. On the other hand, an increase in the surface carbide leads to an increase in the surface hardness and hardened depth (Table 1). Therefore, according to Fig. 7, indirect relations can also be established between the surface hardness or the hardened depth and EC output (Fig. 8). Figure 9 shows the indirect relations between surface hardness, hardened depth and EC output. Regression coefficient of 0·94 indicates that EC technique is a precise method to determine the surface hardness or hardened depth.

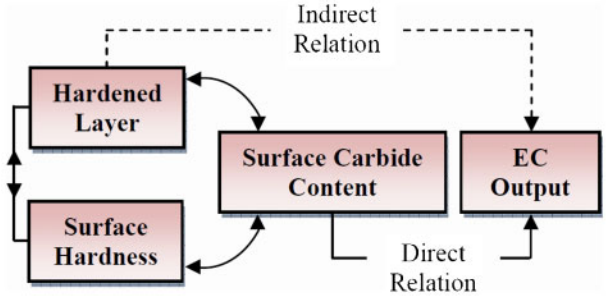

8 Schematic diagram of relation between microstructure, mechanical properties and EC output

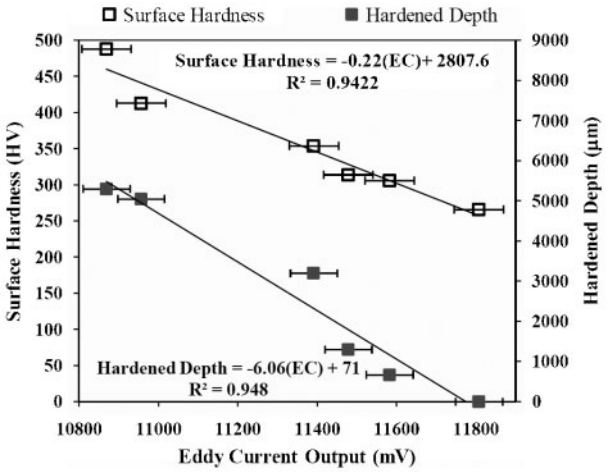

9 Relationships between EC output, surface hardness and hardened depth

Conclusions

In the present research, carbide formation and hardness at the surface of grey cast iron parts were assessed using differential EC method. The relationships between the metallurgical parameters (surface carbide content, surface hardness and case depth) and EC output were also investigated. High correlation coefficients of the relations between EC outputs and metallurgical parameters demonstrate that the proposed non-destructive system provides fast and accurate separation of undesirable parts in mass production lines.

Acknowledgement

This work was supported in part by Ferdowsi University of Mashhad's Research Council under grant no. 16276/2 (dated 17 January 2011).

References

1. G. C. Onwubolu: 'Cutting tool technology', EN 233, lectures in University of the South Pacific, Alofi, Niue, 2006.
2. M. Field and J. F. Kahles: 'Machining characteristics of cast irons', *AFS Trans*., 1954, **62**, 654–659.
3. W. W. Moore and J. O. Lord: 'Gray cast iron machinability – quantitave measurements of pearlite and graphite effects', *AFS Trans*., 1959, **67**, 193–198.
4. ASM International Handbook Committee: in 'Metals handbook', 10th edn, Vol. 1, 'Properties and selection: irons, steels, and high-performance alloys'; 1990, Materials Park, OH, ASM International.
5. D. C. Jiles: *NDT Int.*, 1990, **23**, 83–92.
6. J. García-Martín, J. Gómez-Gil and E. Vázquez-Sánchez: *Sensors*, 2011, **11**, 2525–2565.
7. S. Konoplyuk: *NDT Int.*, 2010, **43**, 360–364.
8. M. Kashefi, S. Kahrobaee and M. H. Nateq: *J. Mater. Eng. Perform.*, 2012, **21**, 1520–1525.
9. S. H. Khan, F. Ali, A. Nusair Khan and M. A. Iqbal: *J. Mater. Process. Technol.*, 2008, **200**, 316–318.
10. F. Habiby, T. N. Siddiqui, S. H. Khan, A. ul Haq and A. Q. Khan: *NDT Int.*, 1992, **25**, 145–146.
11. S. H. Khan, F. Ali, A. Nusair Khan and M. A. Iqbal: *Comput. Mater. Sci.*, 2008, **43**, 623–628.
12. M. Shaira, P. Guy, J. Courbon and N. Godin: *Res. Nondestr. Eval.*, 2010, **21**, 112–126.
13. S. H. Khan, A. Nusair Khan, F. Ali, M. A. Iqbal and H. K. Shukaib: *J. Alloys Compd*, 2009, **474**, 254–256.
14. K. Rajkumar, B. Rao, B. Sasi, A. Kumar, T. Jayakumar, B. Raj and K. Ray: *Mater. Sci. Eng. A*, 2007, **A464**, 233–240.
15. J. Cech: *NDT Int.*, 1990, **23**, 93–102.
16. S. Konoplyuk, T. Abe, T. Uchimoto, T. Takagi and M. Kurosawa: *NDT Int.*, 2005, **38**, 623–626.
17. D. Mercier, J. Lesage, X. Decoopman and D. Chicot: *NDT Int.*, 2006, **39**, 652–660.
18. S. Kahrobaee, M. Kashefi and A. Saheb Alam: *Surf. Coat. Technol.*, 2011, **205**, 4083–4088.
19. X. J. Hao, W. Yin, M. Strangwood, A. J. Peyton, P. F. Morris and C. L. Davis: *Scr. Mater.*, 2008, **58**, 1033–1036.
20. H. Sun, J. R. Bowler, N. Bowler and M. J. Johnson: in 'Review of progress in quantitative nondestructive evaluation', (ed. D. O. Thompson and D. E. Chimenti), Vol. 21, 1561; 2001, Brunswick, Maine (USA), AIP Conference Proceedings.
21. S. Kahrobaee and M. Kashefi: *NDT Int.*, 2011, **44**, 335–338.
22. M. Sheikh Amiri and M. Kashefi: *NDT Int.*, 2009, **42**, 618–621.
23. C. S. Angani, D. G. Park, C. G. Kim, P. Leela, P. Kollu and Y. M. Cheong: *J. Nondestr. Eval.*, 2010, **29**, 248–252.
24. Y. K. Shin, D. M. Choi, Y. J. Kim and S. S. Lee: *NDT Int.*, 2009, **42**, 215–221.
25. D. E. Bray and R. K. Stanley: 'Nondestructive evaluation: a tool design, manufacturing and service'; 1997, Boca Raton, FL, CRC Press.
26. P. J. Shull: 'Nondestructive evaluation: theory, techniques and applications'; 2002, New York, Marcel Dekker Inc.